



The effects of design modifications on the apparent coupling loss factors in SEA-like analysis

A.N. Thite^{a,*}, B.R. Mace^b

^a Department of Mechanical Engineering, School of Technology, Oxford Brookes University, Wheatley, Oxford OX33 1HX, UK

^b Institute of Sound and Vibration Research, University of Southampton, Southampton SO17 1BJ, UK

ARTICLE INFO

Article history:

Received 16 October 2009

Received in revised form

9 June 2010

Accepted 14 June 2010

Handling Editor: Y. Auregan

ABSTRACT

At high frequencies it is often desirable to describe the behaviour of a structure in terms of subsystem energies. The most important method used for high frequency analysis is statistical energy analysis (SEA). Recently, the frequency range in which finite element analysis is applied is being extended to higher frequencies resulting in SEA-like analysis. Methods such as energy distribution modelling can be used to obtain the matrix of energy influence coefficients (EICs); the EIC matrix can be inverted to estimate SEA-like “apparent” coupling loss factors (ACLFs). The ACLFs so estimated depend on details of global modal properties, especially at low and moderate modal overlap. This has implications for design modifications, for example by adding damping treatment to one subsystem, since generally all the EICs change and hence so do all the ACLFs. In principle a full re-analysis is required; this is in contrast to classical SEA. This paper describes these problems and their causes and approximations to the SEA-like parameters of the modified system are proposed. Estimates of the response of the structure after modifications can be found without full re-analysis, leading to a computationally efficient method. The case studies show good agreement between the estimates based on the proposed approaches and the ones based on full re-analysis. The net outcome is that the ACLFs can be estimated after the modification has been made in a manner similar to conventional SEA.

© 2010 Elsevier Ltd. All rights reserved.

1. Introduction

The audio-frequency behaviour of complex engineering structures is of interest in many applications. Energy based modelling approaches are often used to describe this high frequency vibrational behaviour in some average or approximate way. The most important of these is statistical energy analysis [1] (SEA). It provides a statistical approach to modelling physical systems which share gross characteristics but whose properties differ in detail. Finite element (FE) models, on the other hand, are particularly suitable for low frequency vibration analysis but encounter difficulties at higher frequencies, partly because the size of the model becomes increasingly large. FE analysis of parts of a structure can be used to estimate SEA parameters [2–7]. Furthermore, with increasing computer power, the use of FE is being extended to ever-higher frequencies. One consequence of this is the large quantity of output data from a FE model, which makes it difficult for the engineer to judge how best to modify a structure to improve its noise and vibration behaviour. This indeed is one major

* Corresponding author. Tel.: +44 01865484320.

E-mail address: athite@brookes.ac.uk (A.N. Thite).

benefit of SEA: the relative simplicity of the model makes it easier to judge the effects of adding damping or modifying the structure in some other way.

In energy distribution analysis a SEA-like model of a structure is formed with the parameters typically being found from FE of the structure or parts of it. The FE output is post-processed to yield simple energy models in a SEA-like form. One difficulty with this approach, however, is how the effects of design modifications can be predicted without re-analysis of the whole system, which is usually computationally expensive. This is the subject of this paper. The aim is to use the methods described below to estimate, in the first instance, the response after such modifications have been made, with perhaps relatively few re-analyses.

In SEA, the structure is divided into subsystems and the response is described in terms of the total time average subsystem energies \mathbf{E} and input powers \mathbf{P}_{in} . These are, in principle, averages taken over an ensemble of structures whose properties differ in detail and, in practice, are also frequency averages. In a SEA model these powers and energies are related by

$$\mathbf{P}_{in} = \mathbf{L}\mathbf{E} \tag{1}$$

where

$$\mathbf{L} = \omega \text{diag}(\eta_j) + \omega \begin{bmatrix} \eta_{12} + \eta_{13} + \dots & -\eta_{21} & \dots \\ -\eta_{12} & \eta_{21} + \eta_{23} + \dots & \dots \\ \vdots & \vdots & \ddots \end{bmatrix} \tag{2}$$

is a matrix of damping (η_j) and coupling (η_{ij}) loss factors for subsystems i and j and ω is the centre frequency. To maintain energy conservation, the columns of the matrix of coupling loss factors sum to zero. The elements of \mathbf{L} must also satisfy the consistency relation

$$n_i \eta_{ij} = n_j \eta_{ji} \tag{3}$$

where n_i is the (asymptotic) modal density of subsystem i . For a system comprising two subsystems

$$\mathbf{L} = \omega \begin{bmatrix} \eta_1 + \eta_{12} & -\eta_{21} \\ -\eta_{12} & \eta_2 + \eta_{21} \end{bmatrix} \tag{4}$$

Theoretical expressions exist for the CLFs for some circumstances, commonly using a wave approach [1]. Numerical estimates of the CLFs can be obtained from finite element analysis (FEA) of the system [2–7]. The process is essentially a numerical analogue of the power injection method [8] (PIM) which is often used to develop an experimental SEA model of a structure. It broadly involves the following steps: the system is modelled using FEA in a conventional manner, and the mass and stiffness matrices found; the modes of the system are determined; the point response to point, time-harmonic excitation is determined for “many” combinations of excitation and response points; these frequency responses are post-processed by averaging over a chosen frequency band and over the chosen excitation and response points. The result is a matrix of the so-called energy influence coefficients (EICs) \mathbf{A} which relate the subsystem energies and input powers \mathbf{E} and \mathbf{P}_{in} by

$$\mathbf{E} = \mathbf{A}\mathbf{P}_{in} \tag{5}$$

This matrix is then inverted to give

$$\mathbf{P}_{in} = \mathbf{X}\mathbf{E}, \quad \mathbf{X} = \mathbf{A}^{-1} \tag{6}$$

Strictly, the SEA Eq. (1) relates *ensemble average* powers and energies, while the FE predictions \mathbf{X} are based on a *single estimate* of frequency average quantities which depend on the specific input data chosen for the FEA. Thus \mathbf{X} is just an estimate of $\omega\mathbf{L}$, i.e.

$$\mathbf{X} = \omega\hat{\mathbf{L}} \tag{7}$$

The coupling loss factor estimated from a one-off analysis is sometimes referred to as an *apparent coupling loss factor* [5] (ACLF) to distinguish it from ensemble based estimates.

The CLFs in Eq. (1) are independent of subsystem damping. However, it was found in earlier studies [9,10] that CLFs are dependent on damping loss factors at low and moderate modal overlap and hence so are the parameters estimated from Eq. (6). Under these circumstances estimation of ACLFs requires complete knowledge of global modal properties. There are two major concerns in the above approach; one is the robust estimation of parameters such as the ACLFs (i.e. the estimation of parameters which are insensitive to specific details of the structure being analysed and are more representative of the ensemble averages) and the other concerns issues of design modification. The variability of response and parameter estimates tends to be larger for lower modal overlap or if there are relatively few modes in the band [11–13]. Robust estimation methods as in Ref. [14] can be used that give the statistics of the SEA-like parameters. The second issue of design modification has major implications at low and moderate modal overlap. Conventional SEA allows modifications of the structure to be made and the new CLF matrix \mathbf{L} to be found in a straightforward manner. In the EIC approach, however, in principle full re-analysis of the structure is required. This is of course undesirable in practical implementation.

This paper concerns the second issue, i.e. how the effects of modifications to the structure on its energy response can be accurately estimated. Two types of design modifications are considered, with particular reference to the case of a system comprising just two subsystems. The Craig–Bampton component mode synthesis (CMS) approach is used to represent subsystems in terms of their modes. This allows easier implementation of the second approach to design modification.

The first modification concerns addition of damping to one or more of the subsystems. This situation leads to non-proportional damping and issues relating to complex modes. The damping change will have significant effects in the low and moderate modal overlap regions. The modal powers [7,15,16] used to estimate the EICs depend on the damping loss factors which are themselves modified. The behaviour of ACLFs at low modal overlap can be investigated in terms of the modal powers. An approach is proposed to predict modified response due to change in damping without full re-analysis.

The second design modification concerns alteration of connection strength between the subsystems. In terms of the CMS approach, this involves a modification to the interface connecting the subsystems. It is envisaged that one knows the effect of a modification at high modal overlap, and then the issue of its influence at low and moderate overlap is addressed. The design modification of the second type influences both natural frequencies and mode shapes and eventually mode participation factors [15,16]. The average modal density remains the same, i.e. the expected number of modes within a specified excitation band. For a particular modification, this means that the mode participation factors are the ones that determine changes in ACLFs. Here, statistics of the mode participation factors and their variation with respect to change in connection between two subsystems are used to predict the modified response. The approach is then extended to built-up structures for which there are non-zero indirect coupling loss factors.

The characteristic constraint (CC) mode approach that can be used in CMS to reduce the number of interface degrees of freedom (dofs) can also be used to incorporate the modifications. Since the complete statistics of the global modes are necessary to obtain the EICs, full re-analysis of the structure is required. This also means modification of the FE model, computation of the component modes, etc. The aim, however, is to estimate the effects of specific changes involving design modification rather than complete re-analysis, and this involves far less computational cost if CMS and CC modes are used. An approach is proposed where the modified CC modes are used to predict the modified response.

The paper is laid out in the following way. In the next section, expressions for the EICs in terms of the modes of the system are reviewed, following [7,15,16]. The EICs depend on the system's natural frequencies and mode shapes. Fixed interface (Craig–Bampton) component mode synthesis is used to generate global modal parameters. Then the effect of damping modification in a subsystem is analysed and approximate solutions are developed. Later design modifications leading to change in subsystem coupling is discussed and two approximate solutions are proposed and developed. Finally numerical examples are presented.

2. Estimation of EICs

The methods used to calculate the EICs for a system or part of a system are described in detail in Refs. [7,15,16]. In summary, conventional FEA and modal analysis are used to determine the system's mass and stiffness matrices, the natural frequencies and mode shapes. "Rain-on-the-roof" excitation is applied to each subsystem in turn and the energy (strictly twice the kinetic energy) in each subsystem determined. The EIC A_{21} , which relates the energy in subsystem 2 per unit power input to subsystem 1, is given by [14]

$$A_{21} = \frac{E_{\text{rain},21}}{P_{\text{rain},11}} = \frac{\sum_j \sum_k \Gamma_{jk} \psi_{jk}^{(1)} \psi_{jk}^{(2)}}{\sum_j \delta_j \Gamma_{jj} \psi_{jj}^{(1)}} \quad (8)$$

where the subscripts j and k refer to the j th and k th modes of the system. The cross-modal power Γ_{jk} is given by

$$\Gamma_{jk} = \frac{1}{\Omega} \int_{\omega \in \Omega} \frac{1}{4} \omega^2 \beta_{jk}(\omega) d\omega, \quad \beta_{jk} = \text{Re} \left\{ \alpha_j(\omega) \alpha_k^*(\omega) \right\}, \quad \alpha_j = \frac{1}{\omega_j^2 - \omega^2 + i\delta_j \omega} \quad (9)$$

and it depends only on the natural frequencies $\omega_{j,k}$ and bandwidths $A_{j,k}$ of modes j and k . Here, Ω is the frequency band over which the excitation is applied. Broadly, $\Gamma_{jk} \approx 0$ unless both natural frequencies ω_j and ω_k lie in the frequency band of excitation, so that both modes are resonant. The cross-mode participation factor

$$\psi_{jk}^{(1)} = \int_{x \in 1} \rho(x) \phi_j(x) \phi_k(x) dx \quad (10)$$

depends only on the mode shapes within subsystem 1, $\phi_j(x)$ being the j th mode shape, $\rho(x)$ the mass density and the integral being evaluated only over subsystem 1. Further details and discussion can be found in Ref. [15]. Using the inverse of the energy influence coefficient matrix an estimate of the coupling loss factor η_{12} is then obtained from the relation

$$\hat{\eta}_{12} = \frac{1}{\omega} \frac{A_{21}}{A_{11}A_{22} - A_{12}A_{21}} \quad (11)$$

Since the coupling loss factor is based on frequency average quantities for a single system rather than both frequency and ensemble averages, it is referred to here as an apparent coupling loss factor (ACLF) and indicated by $\hat{\eta}_{ij}$.

2.1. A CMS approach to estimating EICs

The SEA-like parameters obtained above using full FE model are not robust in the sense that they provide an estimate based on the specific properties of the chosen system. In Ref. [14], a component mode synthesis (CMS) based solution was proposed which allowed the use of a perturbation method to average over system properties. To carry forward the approach the design modifications have to be implemented based on robust SEA-like parameters. As in Ref. [14], the Craig–Bampton (fixed interface) component mode synthesis [17] is used to estimate global modal properties. The steps are summarised here. Each subsystem is modelled individually (typically using FEA) with the interface fixed and the component normal modes calculated. Constraint modes (associated with the interface degrees of freedom (dofs)) are also included in the model. The individual subsystem models are then assembled and the global eigenvalue problem solved to find the modes of the system as a whole. These modes are used to estimate the baseline response. Full details of this procedure are given in Section 4 of Ref. [7].

After application of CMS the equations of motion of the structure as a whole can be written in the form [17]

$$\mathbf{M}\ddot{\mathbf{q}} + \mathbf{K}\mathbf{q} = \mathbf{0} \tag{12}$$

where the vector of dofs is

$$\mathbf{q} = \begin{Bmatrix} \mathbf{q}_f^{(1)} \\ \mathbf{q}_f^{(2)} \\ \mathbf{q}_c \end{Bmatrix} \tag{13}$$

Here $\mathbf{q}_f^{(1)}$ and $\mathbf{q}_f^{(2)}$ are the fixed interface modal dofs of subsystems 1 and 2, respectively (i.e. the modes when the interface is fixed) while \mathbf{q}_c are the interface physical dofs (associated with motion of the interface nodal dofs). The global mass and stiffness matrices are

$$\mathbf{M} = \begin{bmatrix} \mathbf{I} & \mathbf{0} & \mathbf{m}_{fc}^{(1)} \\ \mathbf{0} & \mathbf{I} & \mathbf{m}_{fc}^{(2)} \\ \mathbf{m}_{fc}^{(1)T} & \mathbf{m}_{fc}^{(2)T} & \mathbf{m}_c \end{bmatrix}, \quad \mathbf{K} = \begin{bmatrix} \text{diag}(\lambda_j^{(1)}) & \mathbf{0} & \mathbf{0} \\ \mathbf{0} & \text{diag}(\lambda_j^{(2)}) & \mathbf{0} \\ \mathbf{0} & \mathbf{0} & \mathbf{k}_c \end{bmatrix} \tag{14}$$

The submatrices in the above equation are diagonal matrices of fixed interface eigenvalues for subsystems 1 and 2, $\text{diag}(\lambda_j^{(1,2)})$ (i.e. the natural frequencies squared when the interface is fixed), coupling mass matrices $\mathbf{m}_{fc}^{(1,2)}$ and constraint mass and stiffness matrices \mathbf{m}_c and \mathbf{k}_c . The remaining matrices (\mathbf{I} and $\mathbf{0}$) represent the identity matrix and matrices of zeros of appropriate dimension. The global eigenvalue problem is then solved, yielding the global eigenvalues λ_k (squares of the natural frequencies) and mode shapes ϕ_k which are then used in Eq. (8) to estimate the EICs [7].

3. Predicting effects of a design modification

Conventional SEA allows modifications of the structure to be made and the new CLF matrix \mathbf{L} to be found in a straightforward manner. In the EIC approach, however, there is a problem in that a change to the structure affects all the modes, and hence all the EICs and hence the inverse of the EIC matrix. In principle this requires full re-analysis of the structure, which is undesirable because of computational cost and time. Instead, it is desirable to develop approximations for the EIC and ACLF matrices of the modified system without full re-analysis. This section contains a brief discussion on design modification and consequent implications of using the EIC matrix for SEA-like parameter estimation.

First it should be noted that if the coupling is weak and the ACLFs estimated from the EICs are good estimates of the ensemble average CLFs, then the resulting model is of a proper SEA form, and there are no significant issues. Changing damping involves amending the diagonal elements of \mathbf{X} (or \mathbf{L}). For modifications affecting the CLFs (or more strictly, the ACLFs), the new values can be estimated either by re-analysis of the connected subsystems alone or by the perturbational technique described below.

Let the structure be modified so that the matrix \mathbf{X} is changed by $\delta\mathbf{X}$. The consequent changes in subsystem energies, $\delta\mathbf{E}$ are such that

$$\mathbf{X}' = \mathbf{X} + \delta\mathbf{X}, \quad \mathbf{E}' = \mathbf{E} + \delta\mathbf{E} = \mathbf{X}'^{-1}\mathbf{P} = \mathbf{A}'\mathbf{P} \tag{15}$$

Using a series expansion of \mathbf{X}'^{-1} and considering only first-order terms, gives

$$\delta\mathbf{E} = \mathbf{X}^{-1}\delta\mathbf{X}\mathbf{E} = \mathbf{A}\delta\mathbf{X}\mathbf{E} \tag{16}$$

The basic issue which needs to be addressed is how to approximate $\delta\mathbf{X}$, without the need to repeat the eigenanalysis of the structure. The use of the SEA-like approach for design modification involves the use of Eq. (16) to predict the modified energy. In classical SEA, where the modal overlap M is large, it is straightforward because only parameters relating directly coupled subsystems will be changed and these are independent of damping. However, if the coupling is strong, there are questions about how the change in coupling loss factor influences, for example, low and moderate modal overlap

applications. The issues are as follows: do we need to modify the FE model? Do we need to re-analyse component modes? Do we need to re-estimate global modal parameters and hence EICs, etc.?

4. Modification to the damping in a subsystem: influence of non-proportional damping on the EICs and ACLFs

Any modifications that change the damping loss factor of a subsystem will result in non-proportional damping of the system under consideration. For estimating the effect of modification one needs to know the implications of this modification on the apparent coupling loss factors in the low and moderate M regions. As it is, one is in principle required to obtain complex modes. However, with the use of the energy distribution model various realistic approximations can be developed. In this section the problem is first stated and then an approximate solution is proposed.

The following discussion concerns two coupled subsystems. In the component mode synthesis representation, assuming that the coupling is conservative, the system damping matrix in local normal modal coordinates is given by

$$\mathbf{\eta}_s = \begin{bmatrix} \mathbf{\eta}_{1t} & 0 & 0 \\ 0 & \mathbf{0} & 0 \\ 0 & 0 & \mathbf{\eta}_{2t} \end{bmatrix} \quad (17)$$

where $\mathbf{\eta}_{it} = \boldsymbol{\phi}_i^T \boldsymbol{\eta}_i \boldsymbol{\phi}_i$ is a diagonal component modal damping matrix. Since the coupling is conservative, for dofs that correspond to the interface the damping loss factors are zero. The above matrix is diagonal and after transformation to global modal coordinates becomes $\mathbf{\eta}_s = \mathbf{P}^T \boldsymbol{\eta}_s \mathbf{P}$. This matrix is also diagonal if the component damping is proportional to the component stiffness matrix. If the damping is non-proportional, the global modal damping matrix can be full and contain significant off-diagonal terms. Here analysis in terms of the global undamped normal modes now involves an approximation. However, especially if the modal overlap is small, one can still use these modes to define an equivalent loss factor for each global mode.

Suppose only hysteretic damping is present. The energy dissipated for hysteretic damping is proportional to the potential energy of the system. For broadband excitation the potential energy can be assumed to be equal to kinetic energy. Consider a system that contains several subsystems each of which have different levels of damping. Within each subsystem, however, the damping is assumed to be proportional to the subsystem stiffness matrix (and/or mass matrix) so that the component normal mode shapes can be used to diagonalise the component damping matrix. The overall or effective damping η_{eff} for each global mode is defined such that

$$V\eta_{\text{eff}} = V_1\eta_1 + V_2\eta_2 + V_3\eta_3 + \dots + V_m\eta_m \quad (18)$$

where V is the potential energy. The subscripts indicate the number of the subsystem. However, the issue is estimating the potential energies in Eq. (18). Using the formulations developed in Ref. [15], the following discussion is developed. The average potential energy of the complete system due to “rain” excitation of component 1 is $V_1 = 2S_f \sum_j \Gamma_{jj} \psi_{jj}^{(1)}$. The modal power Γ_{jj} is dependent on the modal damping. For the self-terms ψ_{jj} , the effective damping loss factor $\eta_{j,\text{eff}}$ is given by

$$\eta_{j,\text{eff}} = \psi_{jj}^{(1)} \eta_1 + \psi_{jj}^{(2)} \eta_2 + \psi_{jj}^{(3)} \eta_3 + \dots + \psi_{jj}^{(m)} \eta_m. \quad (19)$$

This ensures the correct energy dissipation in each subsystem, when the system vibrates in mode j . Using this value for the modal damping loss factor, estimates of the EICs and, ultimately, the ACLFs matrix can be obtained. However, the accuracy of Eq. (19) depends on the relative size of the cross modal terms ψ_{jk} . As a further complicating feature the modal power is not independent of which subsystem is excited. It depends on the modal overlap, which is explained below for a system comprising two subsystems.

The average kinetic energy in subsystem 1, when it is excited, is given by [14]

$$T_{11} = 2S_f \left\{ \sum_j \Gamma_{jj} \psi_{jj}^{(1)2} + \sum_j \sum_{k \neq j} \Gamma_{jk} \psi_{jk}^{(1)2} \right\} \quad (20)$$

and the average kinetic energy in subsystem 2 is then

$$T_{21} = 2S_f \left\{ \sum_j \Gamma_{jj} \psi_{jj}^{(1)} - \sum_j \Gamma_{jj} \psi_{jj}^{(1)2} - \sum_j \sum_{k \neq j} \Gamma_{jk} \psi_{jk}^{(1)2} \right\} \quad (21)$$

Observing Eq. (21), as the modal overlap increases, the third term becomes larger, and eventually cancels out the first two terms. This means that the energy is contained within the first subsystem, which is the excited subsystem. This illustrates the influence of the cross terms in the modal power matrix. The question then arises is what damping values need to be used for estimating the modal powers? It is logical that, under these cases, one needs to use the damping coefficient of the excited subsystem. Thus Eq. (19) is an approximation which is accurate when the modal overlap is small so that cross modal powers can be neglected. For moderate modal overlap, however, bias is introduced by the cross modal powers whose influence becomes significant. What can then be proposed is this: for low modal overlap one can use Eq. (19), for high modal overlap one can use the “normal” SEA procedure and in between some approximations can be used.

4.1. Discussion of approximations at low modal overlap

The changes that can occur at low modal overlap due to non-proportional damping can be explained in terms of the approximations for the EICs. The estimates here are based on the equivalent modal damping of Eq. (19). The following discussion shows how EICs are influenced by changes in damping and eventually lead to changes in the ACLFs.

Again, a system comprising two subsystems is considered. A change in damping results in changes to the modal power matrix. Since the interest is in the low modal overlap region, the discussion will be restricted to the self-terms in the modal power matrix (the diagonal elements Γ_{jj} , since the off-diagonal elements are small). The effects of damping here occur in two ways. The self-terms in the cross modal power [14] are given by

$$\Gamma_{jj} = (1/2\Omega)\text{Re} \left\{ \frac{-\sqrt{-z_j}}{z_j - z_j^*} \arctan \left(\frac{\Omega\sqrt{-z_j}}{\omega_1\omega_2 - z_j} \right) \right\} \tag{22}$$

where $z_j = \omega_j^2(1 - i\eta)$ and $\Omega = \omega_2 - \omega_1$. If the damping bandwidth is small compared to the excitation bandwidth the inverse tangent term above can be approximated as $\pi/2$. For small damping, the real part of the term $(-\sqrt{-z_j}/z_j - z_j^*) \approx 1/2\omega\eta$. With these approximations for low damping one can write the self-terms in the modal power matrix as

$$\Gamma_{jj} \approx \frac{\pi}{8\Omega\omega} \frac{1}{\eta_{\text{eff}}} = \frac{\beta}{\eta_{\text{eff}}} \tag{23}$$

In Eq. (23) β is independent of damping. Then for low modal overlap, based on Eq. (17), the EIC given in (3a) becomes

$$\tilde{A}_{21} \approx \frac{\sum_j (\beta/\eta_{j,\text{eff}}) \psi_{jj}^{(1)} \psi_{jj}^{(2)}}{\sum_j \omega \eta_{j,\text{eff}} (\beta/\eta_{j,\text{eff}}) \psi_{jj}^{(1)}} = \frac{\sum_j \psi_{jj}^{(1)} \psi_{jj}^{(2)} / (\eta_1 \psi_{jj}^{(1)} + \eta_2 \psi_{jj}^{(2)})}{\omega \sum_j \psi_{jj}^{(1)}} = \frac{\sum_j \psi_{jj}^{(1)} \psi_{jj}^{(2)} / (r_\eta \psi_{jj}^{(1)} + \psi_{jj}^{(2)})}{\eta_2 \omega \sum_j \psi_{jj}^{(1)}} \tag{24}$$

where $r_\eta = \eta_1/\eta_2$ is the ratio of the damping coefficient in subsystem 1 to that in subsystem 2. Similarly one can write the other EICs as

$$\tilde{A}_{11} \approx \frac{\sum_j \psi_{jj}^{(1)} \psi_{jj}^{(1)} / (r_\eta \psi_{jj}^{(1)} + \psi_{jj}^{(2)})}{\eta_2 \omega \sum_j \psi_{jj}^{(1)}} \quad \tilde{A}_{12} \approx \frac{\sum_j \psi_{jj}^{(1)} \psi_{jj}^{(2)} / (r_\eta \psi_{jj}^{(1)} + \psi_{jj}^{(2)})}{\eta_2 \omega \sum_j \psi_{jj}^{(2)}} \quad \tilde{A}_{22} \approx \frac{\sum_j \psi_{jj}^{(2)} \psi_{jj}^{(2)} / (r_\eta \psi_{jj}^{(1)} + \psi_{jj}^{(2)})}{\eta_2 \omega \sum_j \psi_{jj}^{(2)}} \tag{25}$$

The estimates based on the above equations can be compared to estimates that are based on a proportional damping model with the damping value equivalent to same average modal overlap as above. Therefore for low modal overlap, for example, one of the EICs reduces to

$$A_{11} \approx \frac{\sum_j \psi_{jj}^{(1)} \psi_{jj}^{(1)}}{\eta_{\text{eff}} \omega \sum_j \psi_{jj}^{(1)}} \tag{26}$$

If $r_\eta - 1$ there are no significant differences between Eqs. (25) and (26). The other two case, $r_\eta \ll 1$ and $r_\eta \gg 1$, are considered in the discussion below.

4.1.1. Apparent coupling loss factor for $r_\eta \ll 1$

In this case $\eta_1 \ll \eta_2$. From Eq. (25), the largest contributions to \tilde{A}_{11} come from those modes for which the participation factors $\psi_{jj}^{(1)}$ are large. Due to orthogonality, when $\psi_{jj}^{(1)}$ is large $\psi_{jj}^{(2)}$ will be small (since $\psi_{jj}^{(1)} + \psi_{jj}^{(2)} = 1$). As the damping coefficient ratio r_η is substantially less than 1, the term in parenthesis is smaller than 1, hence the contribution from such a mode increases accordingly. The contribution from those modes for which $\psi_{jj}^{(1)}$ is small does not change much. In essence, \tilde{A}_{11} is thus greater than the value of A_{11} given by Eq. (26).

Conversely, the contributions to \tilde{A}_{22} from modes for which $\psi_{jj}^{(2)}$ is large is hardly altered by changing the damping. The modes for which $\psi_{jj}^{(2)}$ is small have increased contributions. Overall, the increase seen here is not as large as that for \tilde{A}_{11} .

The cross terms are significant only when both modal participation factors are significant i.e. the mode is participating strongly in both subsystems. As both $\psi_{jj}^{(1)}$ and $\psi_{jj}^{(2)}$ are close to 0.5 for such modes, the increase in these cross terms are small compared with those of \tilde{A}_{22} and A_{11} . In summary, $\delta\tilde{A}_{11} > \delta\tilde{A}_{22}$, $\delta\tilde{A}_{11} > \delta\tilde{A}_{12}$ or $\delta\tilde{A}_{21}$ and $\delta\tilde{A}_{22} > \delta\tilde{A}_{12}$ or $\delta\tilde{A}_{21}$. Based on these variations, the increase in the denominator of Eq. (11) is larger than that in the numerator and hence the apparent coupling loss factors decrease.

4.1.2. Apparent coupling loss factor for $r_\eta \gg 1$

Similar to the above case, the contributions to \tilde{A}_{11} that come from the modes for which the participation factors $\psi_{jj}^{(1)}$ is large hardly changes. The modes with smaller $\psi_{jj}^{(1)}$ give increased contributions. The overall increase is not very significant. However, $\tilde{A}_{11} > A_{11}$, with A_{11} being given by Eq. (26).

The contributions to \tilde{A}_{22} from modes with large participation factors $\psi_{jj}^{(2)}$ increase significantly as the denominator in the parenthesis becomes small. The increases in the contribution of modes with smaller values of $\psi_{jj}^{(2)}$ is significant. Overall, the increase seen here is much larger than that seen in \tilde{A}_{11} .

As in the earlier case, the increases in the cross terms are much less than those of both \tilde{A}_{22} and \tilde{A}_{11} . In summary, $\delta\tilde{A}_{22} > \delta\tilde{A}_{11}$, $\delta\tilde{A}_{11} > \delta\tilde{A}_{12}$ or $\delta\tilde{A}_{21}$ and $\delta\tilde{A}_{22} > \delta\tilde{A}_{12}$ or $\delta\tilde{A}_{21}$. As before, based on these changes in the parameters, the

increase in denominator of Eq. (11) is larger than that of the numerator and hence the apparent coupling loss factors decrease.

The above discussions show that it does not matter to which subsystem the damping is added, the relative amount of power transmitted between subsystems is always smaller compared to the original system with proportional damping. This is in accordance with conclusions drawn from a conventional SEA model.

5. Design modification by changing CLFs

Modifications to the structure which involve changing the structural connections between various subsystems would lead to changes in both natural frequencies and mode shapes. The average modal density remains the same, but the mode participation factors $\psi_{jk}^{(i)}$ (Eq. (10)), however, will change and so, too, do the EICs. To determine the exact effects of such modifications one needs, in principle, a full calculation of the global modal parameters from the modified FE model. However, one would like to be able to estimate the effects of such changes without performing a full re-analysis. Some approaches are suggested in this section that approximate changes to the matrix \mathbf{X} for such changes in the connection between subsystems. In the following section the influence of these changes on mode participation factors and ACLFs is discussed. Then the approach is extended to a system comprising 3 subsystems. An alternative is also proposed which exploits simplification and reduction that arises using characteristic constraint (CC) modes in a CMS model.

5.1. Influence of participation factors

In the low modal overlap region, it was shown in Ref. [16] that the coupling loss factors are dependent on the first two moments of the mode participation factor statistics. The first moment is, however, only dependent on the relative modal densities of the subsystems. In the case of a change in coupling, this will not change. What remains is the variance of the mode participation factors. If one is able to estimate the change in this with respect to changing connection between subsystems, changes to the apparent coupling loss factors can be estimated straightforwardly. The discussion below, which is given in terms of the influence of the power transmission ratio on mode participation factors, gives some understanding of the variation of this statistic.

Again, consider a system with 2 components. Assuming a constant modal bandwidth the power transmission ratio, defined as the ratio of the transmitted power to the input power, can be written in terms of the modal power and modal participation factors as

$$r_{12} = \frac{P_{12}}{P_{in}} = \frac{1}{\sum_j \Gamma_{jj} \psi_{jj}^{(1)}} \left\{ \sum_j \Gamma_{jj} \psi_{jj}^{(1)} \psi_{jj}^{(2)} - \sum_j \sum_{k \neq j} \Gamma_{jk} \psi_{jk}^{(1)2} \right\} \quad (27)$$

For any given connection strength, due to orthogonality, $\psi_{jj}^{(1)} + \psi_{jj}^{(2)} = 1$ and $\psi_{jk}^{(1)} + \psi_{jk}^{(2)} = 0$. This results in $\sigma_0^2 = \text{Var}[\psi_{jj}^{(r)}]$, $\sigma_k^2 = \text{Var}[\psi_{jj+k}^{(r)}]$ and $\overline{\psi_{jj+k}^{(r)}} = 0$ for $k=1,2,\dots,n$. From [15]

$$\Gamma_{jk} \approx \Gamma_{jj} M_{jk}^2 / (M_{jk}^2 + 1) \quad (28)$$

where M_{jk} is the modal overlap of modes j and k , and is defined as the ratio of the damping bandwidth to the modal spacing. For large modal overlap, approximating the natural frequencies as being equally spaced does not give rise to significant errors. Given this assumption, the above relation simplifies to

$$r_{12} = \frac{1}{\sum_j \psi_{jj}^{(1)}} \left\{ \sum_j \psi_{jj}^{(1)} \psi_{jj}^{(2)} - \sum_j \sum_{k \neq j} \frac{M^2}{M^2 + (j-k)^2} \psi_{jk}^{(1)2} \right\} = \frac{1}{v_1} \left\{ v_1 v_2 - \sigma_0^2 - \sum_k^{N-m} \frac{M^2}{M^2 + k^2} \sigma_k^2 \right\} \quad (29)$$

For a special case of no connection between the two subsystems $r_{12}=0$; due to orthogonality of mode shapes $\psi_{jj}^{(r)} = 1$ and $\psi_{jk}^{(r)} = 0$. This results in $\sigma_0^2 = \text{Var}[\psi_{jj}^{(r)}] = v_1 v_2$, where

$$v_1 = \frac{1}{n} \sum_{j=1}^n \psi_{jj}^{(1)} \quad \text{and} \quad v_2 = \frac{1}{n} \sum_{j=1}^n \psi_{jj}^{(2)} \quad (30)$$

are the fractional modal densities of the two subsystems and $\sigma_k^2 = \text{Var}[\psi_{jj+k}^{(r)}] = 0$ for $k=1,2,\dots,n$.

Therefore, for any other connection between subsystems, σ_0^2 decreases as the power transmission ratio increases but σ_k^2 , the variances of cross modal participation factors, increases. As the coupling loss factor is proportional to the power transmission ratio, it decreases as the variance of the mode participation factors increases.

If in design modification one is interested in reducing the power transmitted between the two subsystems, or equivalently reducing the coupling loss factors between them, it is possible that the variances may change gradually to approach the extreme values applicable for no connection. Later, a series of numerical analyses are performed on a system comprising two subsystems; the results are presented Section 6.

5.2. Effect on indirect coupling loss factors due to a change in coupling

The presence of subsystems that are not physically connected together can have some influence on the estimated apparent coupling loss factors. This influence results in the so-called indirect coupling loss factors (ICLFs). At low modal overlap, and for interface conditions resulting in strong connection, these ICLFs can be large and significant. The accurate estimation of design modifications remains problematic in these systems as well; any change in connection will have an effect on the indirect coupling loss factors. Exploiting the discussion developed in the last section, the concept can be extended to include the effects of indirectly connected subsystems. In terms of participation factors, this situation arises due to the correlation between participation factors of indirectly connected subsystems. The EICs can again be written in terms of the statistics of the mode participation factors. When there are three or more subsystems the variances and covariances of the mode participation factors of all the subsystems are related. Considering a system comprising of three subsystems (where subsystems 1 and 3 are indirectly connected), in the low modal overlap region the EIC matrix can be written as

$$\mathbf{A} \approx \frac{1}{\omega\eta} \begin{bmatrix} v_1^2 + \sigma_{0,1}^2 & v_1 v_2 + \rho_{0,12} & v_1 v_3 + \rho_{0,13} \\ v_1 v_2 + \rho_{0,12} & v_2^2 + \sigma_{0,2}^2 & v_2 v_3 + \rho_{0,23} \\ v_1 v_3 + \rho_{0,13} & v_2 v_3 + \rho_{0,23} & v_3^2 + \sigma_{0,3}^2 \end{bmatrix} \begin{bmatrix} v_1 & 0 & 0 \\ 0 & v_2 & 0 \\ 0 & 0 & v_3 \end{bmatrix}^{-1} \tag{31}$$

where $\sigma_{0,p}$ is the variance of the self-participation factors $\psi_{jj}^{(p)}$ in subsystem σ_0 , and $\rho_{0,pq}$ is the covariance of the self-participation factors $\psi_{jj}^{(p)}$ and $\psi_{jj}^{(q)}$. To estimate the change $\delta\mathbf{X}$ that results from a change in the system properties, one needs knowledge of the changes in the variances and covariances of the participation factors. The process of estimating $\delta\mathbf{X}$ can be made simpler by assuming that the covariance of the participation factors of two subsystems does not change as long as the connection between them or through another subsystem does not change. For example if the coupling between subsystem 1 and 2 is changed, the assumption is that ρ_{23} will remain the same. The following discussion allows re-estimation of the covariances of the participation factors without the need to repeat the eigenanalysis.

From the definition of the modal participation factors and due to mode shape orthogonality,

$$\psi_{jj}^{(1)} + \psi_{jj}^{(2)} + \psi_{jj}^{(3)} = 1 \tag{32}$$

The variance of the participation factors in subsystem 1 is given by

$$\sigma_{0,1}^2 = \text{Var}[\psi_{jj}^{(1)}] \tag{33}$$

Substituting Eq. (32) in Eq. (33) it follows that

$$\sigma_{0,1}^2 = \text{Var}[(1 - \psi_{jj}^{(2)} - \psi_{jj}^{(3)})] \tag{34}$$

and by using the relation $v_1 + v_2 + v_3 = 1$ it follows that

$$\sigma_{0,1}^2 = E\left[\left\{ (v_2 - \psi_{jj}^{(2)}) + (v_3 - \psi_{jj}^{(3)}) \right\}^2\right] = \sigma_{0,2}^2 + \sigma_{0,3}^2 - 2v_2 v_3 + 2E[\psi_{jj}^{(2)} \psi_{jj}^{(3)}] \tag{35}$$

Similarly one can write

$$\sigma_{0,2}^2 = \sigma_{0,1}^2 + \sigma_{0,3}^2 - 2v_1 v_3 + 2E[\psi_{jj}^{(1)} \psi_{jj}^{(3)}], \quad \sigma_{0,3}^2 = \sigma_{0,1}^2 + \sigma_{0,2}^2 - 2v_1 v_2 + 2E[\psi_{jj}^{(1)} \psi_{jj}^{(2)}] \tag{36}$$

These statistics of the participation factors can be easily estimated from the baseline analysis (e.g. [14]). The extreme case of no connection can also be explored as in Section 5.1. If subsystem 1 is disconnected from subsystems 2 and 3, based on the fractional modal densities for the case of no connection, $\sigma_{0,1}^2 = v_1(v_2 + v_3)$. This also leads to restrictions on the covariances such that

$$\rho_{0,1(2+3)} = \text{cov}(\psi_{jj}^{(1)}, \psi_{jj}^{(1)} + \psi_{jj}^{(3)}) = \rho_{0,12} + \rho_{0,13} = -v_1(v_2 + v_3) \tag{37}$$

Assuming that the ratio of covariances $\rho_{0,12}/\rho_{0,13}$ remains approximately the same before and after disconnection of subsystem 1, the covariances can be estimated. This assumption is based on the fact that the coupling between subsystems 2 and 3 is not changing. Now the last term in Eq. (36) can be written as

$$E[\psi_{jj}^{(1)} \psi_{jj}^{(3)}] = v_1 v_3 + \rho_{0,13}, \quad E[\psi_{jj}^{(1)} \psi_{jj}^{(2)}] = v_1 v_2 + \rho_{0,12} \tag{38}$$

From Eq. (35), due to the assumption that the changes in the covariances are small, $E[\psi_{jj}^{(2)} \psi_{jj}^{(3)}]$ can be written in terms of the corresponding variances. Therefore it follows that

$$\sigma_{0,2}^2 = \sigma_{0,1}^2 + \sigma_{0,3}^2 + 2\rho_{0,13}, \quad \sigma_{0,3}^2 = \sigma_{0,1}^2 + \sigma_{0,2}^2 + 2\rho_{0,12} \tag{39}$$

One can then use Eqs. (36) and (39) to form simultaneous equations and obtain $\sigma_{0,2}^2$ and $\sigma_{0,3}^2$. As earlier, for design modification it can be suggested that the variances reach extreme values gradually from baseline estimates and so do the covariances. A similar discussion as in Section 5.1 can be developed to illustrate the dependence of changes to the ACLFs and their effect on the statistics of participation factors.

5.3. Incorporating a change in coupling using a CMS approach

The effects of design modifications involving a change in the connection between subsystems can also be estimated using FEM and CMS. The numerical model can be further reduced if the characteristic constraint (CC) modes [18] approach is used. These modes can be obtained by a secondary modal analysis of the interface-related mass and stiffness matrices $\rho_{0,13}\mathbf{m}_c$ and \mathbf{k}_c . Then changes to the interface properties lead to changes in the CC modes and only a re-analysis of the global matrices is required for estimation of the modified participation factors. In what follows, a brief introduction is given to the approach used in calculating the CC modes. Later a relationship is established between the CC modes and the transmitted power and eventually the power transmission ratio. An approach is suggested where the CC modes are incrementally changed to obtain changes in connection between subsystems. The change due to addition of stiffeners (e.g. a beam) on the interface is illustrated in Section 6.

5.4. Characteristic constraint modes

In Ref. [18], a secondary eigenvalue analysis of the constraint mode partitions of the mass and stiffness matrices \mathbf{m}_c and \mathbf{k}_c is carried out to reduce the CMS model size. The eigenvectors obtained are called characteristic constraint modes. The characteristic constraint modes yield physical insight into the mechanisms of vibrational energy transmission across interfaces in complex structures. The first few CC modes were seen to contribute most of the power flow between the components; hence the modes may be truncated without loss of accuracy. Here, in addition to the reduced order model that is achieved, the dependence of the power transmission ratio on the CC modes is explored. The connection between subsystems can be modified by changing the CC modal properties. The alteration can be related to changes in mass or stiffness at the interface. Thus it is easy to incorporate interface changes that have physical meaning.

The CC modes can be obtained by posing an eigenvalue problem for the constraint mode partitions of the CMS matrices [18]:

$$\mathbf{k}_c \boldsymbol{\theta}_{cc} = \lambda_{cc} \mathbf{m}_c \boldsymbol{\theta}_{cc} \quad (40)$$

Solving the eigenvalue problem and transforming the equations of motion into these modal coordinates results in transformed inertial coupling matrices, a diagonal CC modes matrix and an identity matrix for the interface mass matrix. The global mass and stiffness matrices become

$$\mathbf{M} = \begin{bmatrix} \mathbf{I} & \mathbf{0} & \mathbf{m}_{fc}^{(1)} \boldsymbol{\Theta} \\ \mathbf{0} & \mathbf{I} & \mathbf{m}_{fc}^{(2)} \boldsymbol{\Theta} \\ \boldsymbol{\Theta}^T \mathbf{m}_{fc}^{(1)T} & \boldsymbol{\Theta}^T \mathbf{m}_{fc}^{(2)T} & \mathbf{I} \end{bmatrix}, \quad \mathbf{K} = \begin{bmatrix} \text{diag}(\lambda_j^{(1)}) & \mathbf{0} & \mathbf{0} \\ \mathbf{0} & \text{diag}(\lambda_j^{(2)}) & \mathbf{0} \\ \mathbf{0} & \mathbf{0} & \text{diag}(\lambda_j^{cc}) \end{bmatrix} \quad (41)$$

$\boldsymbol{\Theta} = [\boldsymbol{\theta}_{cc1}, \boldsymbol{\theta}_{cc2}, \dots]$ is the matrix of CC eigenvectors. In the above equation both component and CC modes can be truncated.

5.5. Power transmission and CC modes

The time average power transmitted from subsystems 1 to 2 for a time harmonic excitation is given by

$$P_{12} = \frac{1}{2} \text{Re} \{ \mathbf{v}_1^c \mathbf{F}_t \} \quad (42)$$

where \mathbf{F}_t is a vector of traction forces on the interface dofs and \mathbf{v}_1^c is a vector of corresponding velocities. The above equation can be written in terms of component modal properties and the interface characteristic constraint modes [19]. The vector of velocities can be transformed to CC modal coordinates by using corresponding mode shape matrix as

$$\mathbf{v}_1^c = \boldsymbol{\Theta} \mathbf{v}_1^{cc} \quad (43)$$

where \mathbf{v}_1^{cc} is a vector of CC modal velocities. By using the equations of motion of component 1 and incorporating the dynamic effect of the presence of component 2 by traction forces, the CC modal velocities are obtained as

$$\mathbf{v}_1^{cc} = \mathbf{Y}_{12}^{\boldsymbol{\Theta}} \boldsymbol{\Theta}^T \mathbf{f}_1 \quad (44)$$

where

$$\mathbf{Y}_{12}^{\boldsymbol{\Theta}} = \{ \boldsymbol{\Theta}^T (\mathbf{Z}_1 + \mathbf{Z}_2) \boldsymbol{\Theta} \}^{-1}; \quad \mathbf{f}_1 = \mathbf{f}_c^{(1)} - j\omega \mathbf{m}_{fc}^{(1)} \mathbf{z}_{ff}^{(1)-1} \mathbf{f}_f^{(1)}; \quad \mathbf{Z}_i = \mathbf{z}_c^{(i)} + \omega^2 \mathbf{m}_{fc}^{(i)} \mathbf{z}_{ff}^{(i)-1} \mathbf{m}_{fc}^{(i)T} \quad (i = 1, 2) \quad (45)$$

The vector of traction forces is given by

$$\mathbf{F}_t = \mathbf{Z}_1 \boldsymbol{\Theta} \mathbf{v}_1^{cc} - \mathbf{f}_1 \quad (46)$$

where \mathbf{z}_c^i is an impedance matrix of component i associated with the characteristic constraint modes, \mathbf{z}_{ff}^i is an impedance matrix of component i associated with component normal modes, $\mathbf{f}_f^{(1)}$ is a vector of forces on subsystem 1 transformed to component modal coordinates and $\mathbf{f}_c^{(1)}$ is a vector of forces acting on the interface of components 1 and 2.

Close observation of Eqs. (40)–(44) reveals the relation between the transmitted power and combination of CC modes and the component normal modes. The power transmission can be written as

$$P_{12} = P_{12} \left(\frac{\lambda_1}{\lambda_{cc,1}}, \frac{\lambda_2}{\lambda_{cc,1}}, \dots, \frac{\lambda_1}{\lambda_{cc,2}}, \frac{\lambda_2}{\lambda_{cc,2}}, \dots, \phi, \theta, f_c, f_f, m_f \right) \quad (47)$$

Increases in the CC modal eigenvalues reduce the power transmitted compared with the baseline case. This also is an indicator of degree of impedance mismatch at the interface. The impedance mismatch leading to an increase in CC eigenvalues can be achieved by, for example, stiffening the interface by a beam stiffener or springs, etc. For some modification of coupling, the input power does not change.

For small or moderate changes about the nominal design point, an approximation for the power transmission ratio can be developed. Further, assuming that all CC eigenvalues increase proportionally, the power transmission ratio can be written in terms of only the first CC eigenvalue. Therefore, for any change in the interface that does not affect the component modes and the CC eigenvectors, the power transmission ratio can be written as

$$\log(r_{12}) \approx a - b \log(\omega_{cc,1}) \quad (48)$$

where a and b are constants which represent the influence of all parameters other than CC eigenvalues. Note that the cases where $\omega_{cc,1} = 0$ are not considered in this study.

The value of b in Eq. (48) very much depends on the subsystems and the interface parameters. For a design modification knowledge of the constants b and a are required so that any change in coupling can be related to changes in the ACLF and then to changes in the CC modes. To estimate this slope a perturbation approach can be used to relate global modal statistics for small change in the CC modes. These global modal properties can be used to estimate the EICs and CLFs. Consequently the parameters a and b can be estimated. The details of the perturbation approach are given in Ref. [20] and its application to robust CLF estimation is given in Ref. [14].

6. Numerical examples

In this section, numerical examples for systems comprising two edge-coupled plates are presented. The plates are the same as those considered in Ref. [12]. The baseline values of the properties of the plates are given in Table 1. The plates have straight edges and all edges, including the line of coupling, are simply supported. The plates have one of two different shapes, giving two systems whose only difference is the shape of the subsystem plates, and hence which have different modes and mode spacing statistics. Both plates are either rectangular (RR) or pentagonal (PP) in shape (as shown in Fig. 1) allowing investigation of different amounts of irregularity. ANSYS shell elements of Type 63 were used for the FEA with an element edge length of 0.05 m. Only the dofs corresponding to flexural motion were retained. “Rain-on-the-roof” excitation was assumed. The baseline, discrete frequency estimates were made using CMS with the baseline mass and stiffness properties in Table 1.

6.1. Non-proportional damping

Fig. 2 shows the ACLF for 3 cases of damping. In estimating the ACLFs a frequency band of 400 Hz is used with a centre frequency of 1500 Hz, with the bandwidth of excitation containing 27 modes on average. For subsystems that have the same damping loss factor, the ACLF variation is dependent on the modal overlap M . Note that the modal overlap is calculated based on the effective modal damping loss factor (Eq. (19)). The ACLF is proportional to the damping loss factor at low M and as M increases it asymptotes to a constant value. This asymptote can also be obtained by other approaches used in obtaining SEA parameters, such as the wave approach. For the two cases where non-proportional damping is used, at low modal overlap the coupling loss factors are smaller than when the damping is the same in both subsystems (this observation is in accordance with the discussion in Section 4.1). In both cases, when the subsystems that have a smaller damping are excited, the modal energy of the excited subsystem becomes relatively larger compared to the non-excited subsystem as discussed earlier. This results in a smaller proportion of the input power being transmitted to the non-excited systems in general. The non-proportional damping based estimates do not asymptote to the value obtained using same damping loss factors at high modal overlap. The deviations are due to the use of the effective modal damping loss factor in estimating ACLFs, which was shown in Section 4 to result in good approximations only at low modal overlap.

Table 1

Physical and geometric properties (SI units) for plates 1 and 2.

Physical and geometric properties (SI units) for plates 1 and 2			
Elastic modulus	2×10^{11}	Length of coupled edge	0.9
Density	8×10^3	Plate area (1, 2)	0.9, 1.26
Poisson's ratio	0.3	Modal density (1, 2)	0.0297, 0.0416
Thickness	0.01	System total modal density	0.0714

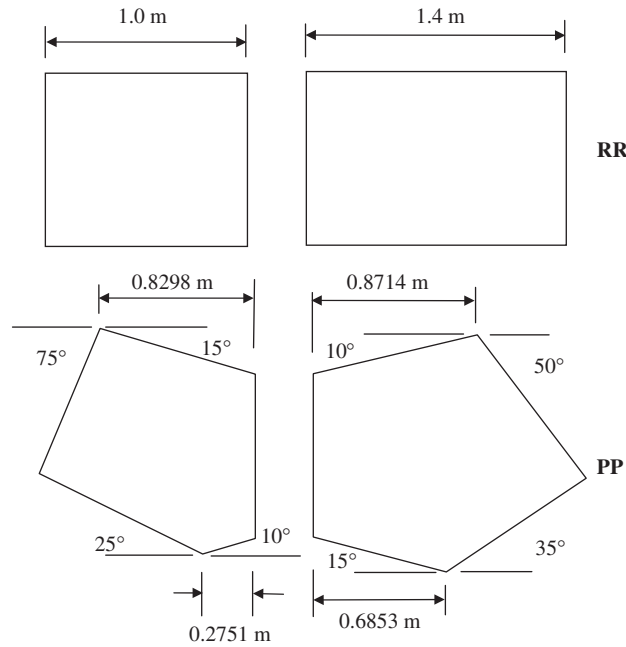


Fig. 1. Rectangular (RR) and pentagonal (PP) plates used in numerical simulations.

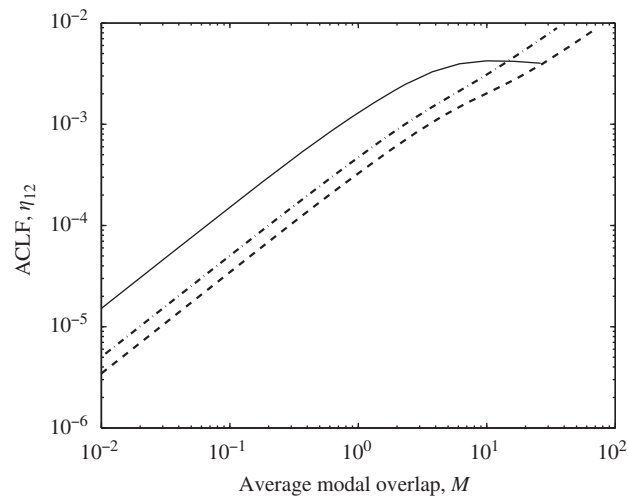


Fig. 2. ACLF variation against average modal overlap. — $\eta_1/\eta_2=1$, - - - $\eta_1/\eta_2 \ll 1$ and - · - · - $\eta_1/\eta_2 \ll 1$.

In summary, if the damping loss factors of the two subsystems are different, then the ACLFs are less than if the damping were the same in all subsystems for the same average modal overlap factor. The approximate change in the apparent coupling loss factor can be estimated without full recalculation for low values of M . There is no need for re-analysis for large damping loss factor, which is in general associated with large values of M , where asymptotic estimates of coupling loss factors are available. However, for moderate M interpolation can be used to estimate the apparent coupling loss factors. Fig. 3 shows this approximation. Here a frequency band of 400 Hz is used with a centre frequency of 600 Hz and the bandwidth of excitation contains 27 modes on average.

6.2. Change in connection between subsystems

6.2.1. Influence of variance of participation factors

Here, results of numerical experiments performed on rectangular and pentagonal plates to assess the influence of length of the coupled edge and hence the coupling connection strength on the power transmission ratio and, in turn, on

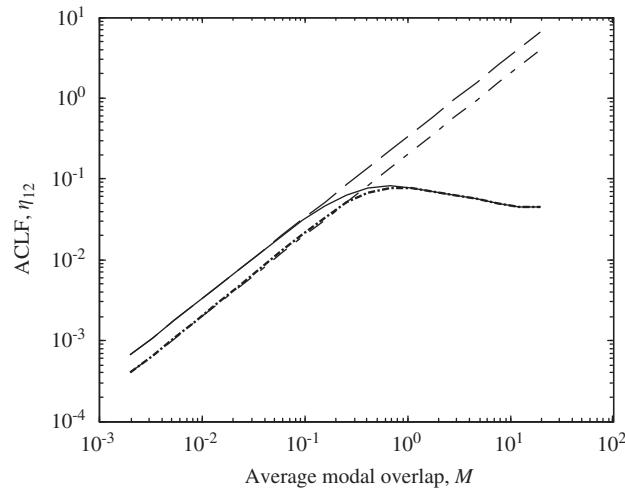


Fig. 3. Approximate ACLF variation against average modal overlap. — $\eta_1/\eta_2=1$ and - - - $\eta_1/\eta_2 \ll 1$. Also shown are respective low modal overlap approximations — — — and — — — —.

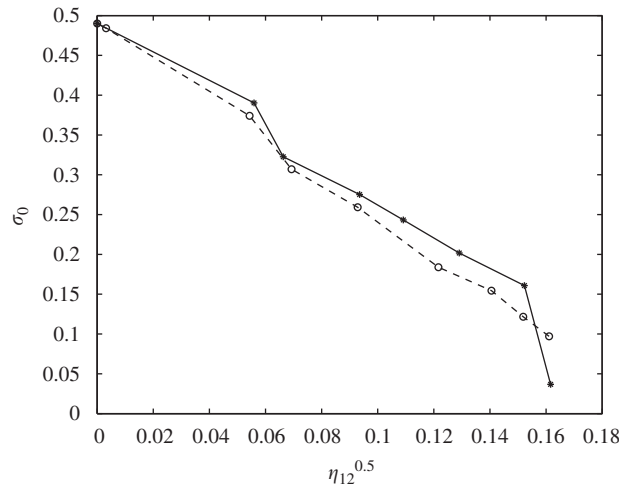


Fig. 4. Variation of standard deviation of participation factors as a function of CLF. — RR plates and - - - PP plates.

mode participation factor statistics are given. The coupling length is varied by preventing rotation and out of plane displacement for different numbers of nodes on the interface. A frequency band of 400 Hz is used with a centre frequency of 600 Hz. The bandwidth of excitation contains 27 modes on average.

Fig. 4 shows the standard deviation σ_0 of the modal participation factors ψ_{ij} as a function of ACLF. For the PP plates the relation is approximately linear. For RR and PP cases σ_0^2 is approximately inversely proportional to η_{12} . The standard deviation is maximum when $\eta_{12}=0$ and is then equal to $\sqrt{v_1 v_2}$. This linear behaviour allows an interpolation to be made of the ACLF as a function of the length of the coupled sides of the plates.

In summary, for design modification involving a change in connection between subsystems one can estimate the change in ACLF using other approaches to SEA parameter estimation (for example, the wave approach). The ACLF so estimated can then be related to the change in the standard deviation of the participation factors. This allows estimation of low modal overlap changes in ACLF. For moderate modal overlap one can use an approximation based on the low and moderate modal overlap estimates. The net outcome is that one can modify the coupling loss factors in a manner similar to conventional SEA. The modifications obtained, however, may not be very accurate for regularly shaped structures.

6.2.2. Interface modification and CC mode analysis

The results based on concepts from Sections 5.3 to 5.5 are presented here; two numerical experiments were performed on RR plates. The centre frequency used is 1500 Hz with a bandwidth of 400 Hz. In the first case the connection between subsystems is varied by the introduction of a beam on the interface. The cross section of the beam is varied to achieve

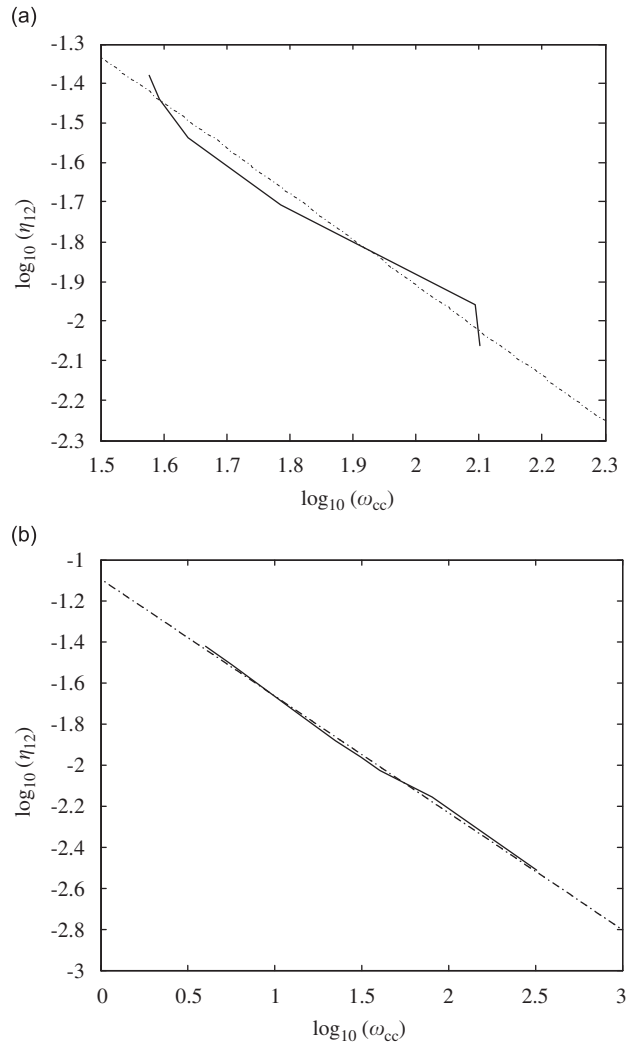


Fig. 5. Variation in CLF as a function fundamental CC mode: (a) — beam stiffer and — · — · — approximate fit (all edges are simply supported), (b) — spring stiffer and — · — · — approximate fit (two adjacent edges to interface are free and other edges are simply supported).

varying connection strength between the subsystems. The width of the beam is 0.05 m and the height is varied from 0.001 to 0.12 m to obtain varying stiffness. The power transmission decreases as the beam stiffness increases. The coupling is strongest without the beam present. In modifying the connection, the CC natural frequencies also change. The variation of the fundamental CC natural frequency as a function of ACLF is plotted in Fig. 5a. There is an approximate linear dependency of $\log(\hat{\eta}_{12})$ on $\log(\omega_{cc})$ as indicated by Eq. (48). This implies that interpolation between two known points can be used to inform the effects of stiffening the connection between two subsystems.

A different case is shown in Fig. 5b. Here rotational springs are introduced along the coupled edge. The boundary conditions are different: two edges adjacent to the interface are free and the other two edges are simply supported. This example was chosen to verify the behaviour for different boundary conditions which can have significant impact on global modal behaviour which affects low M ACLF estimates. Fig. 5b shows the ACLF as a function of the fundamental CC natural frequency. Again the relation follows approximately a linear behaviour.

Based on the relation between the CC modes and the ACLF one can estimate the ACLFs after modification by just performing one global modal analysis. Here two such cases are validated; the connection between the two subsystems is modified by the addition of beam stiffeners (0.03 and 0.04 m height, respectively, width being 0.05 m). Fig. 6a shows the variation of the ACLF as a function of the modal overlap M . Estimates based on both full re-analysis and approximation are shown. The approximate estimate is based on changing the CC natural frequency to give a new estimate of the ACLF. The estimates agree well with those obtained by complete re-analysis. Fig. 6b shows corresponding results for the example of Fig. 5b. The spring stiffness used is 2.31×10^4 N m/rad. Here again the estimate found by changing the CC natural frequencies is in good agreement with that of the full re-analysis.

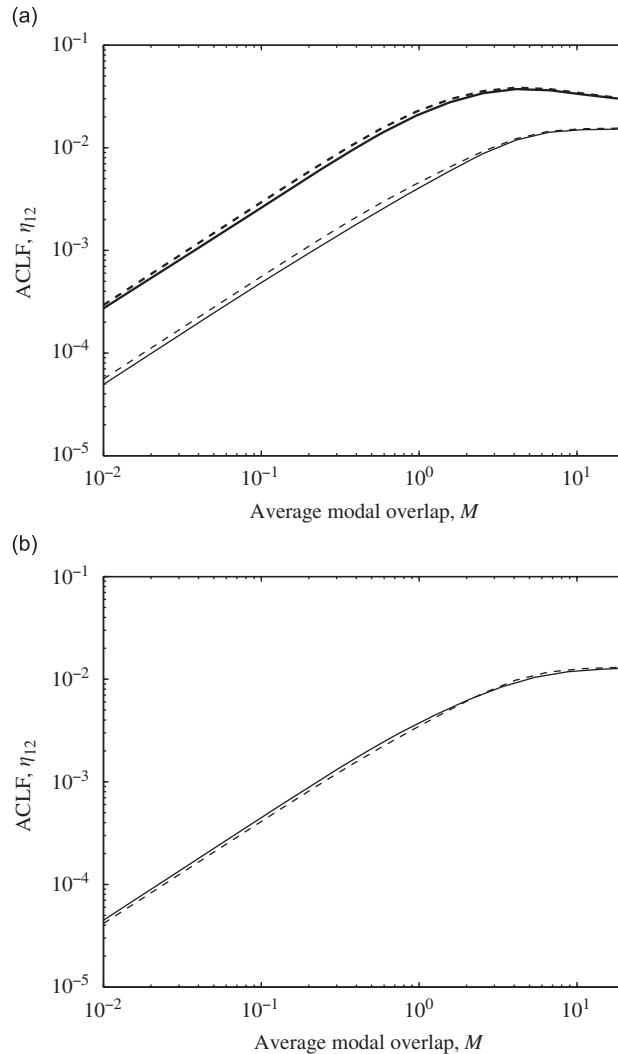


Fig. 6. Validation of coupling modification by change in CC modes (a) addition of beam stiffener of width 0.05 m: ——— beam stiffener of 0.04 m height and - - - - modified CC modes; ——— beam stiffener of 0.03 m height and - · · · · · modified CC modes (b) addition of springs: ——— additional springs and - - - - modified CC modes.

Design modification involving change in the connection between two subsystems results in changes in the modal participation factor statistics as noted earlier. The advantage of the approach in which CC natural frequencies are modified is that one can obtain estimate of the statistics of participation factors. These then can be used to obtain robust SEA-like parameters.

7. Conclusions

In SEA-like analysis, a FE model of a structure or part of the structure is formed, a global eigenvalue analysis is performed and the results processed to form an energy model, yielding the so-called apparent coupling loss factors (ACLFs). The issue addressed in this paper was how the effects of modifications to the structure can be estimated without the need for multiple full re-analysis. Changes might be made in either damping or the coupling between subsystems.

In modifications involving changes to the damping approximate changes in the ACLFs can be estimated without complete re-analysis for low M . However, for moderate M one can use interpolation to obtain estimates of the ACLFs. For small to moderate changes in connection between subsystems about a design point, the changes in the ACLFs can be estimated by knowing the changes in modal participation factor statistics. Alternatively the approach of modified CC natural frequencies can be used in estimating ACLFs. The case studies show good agreement between the estimates based on the proposed approaches and the ones based on full re-analysis. The net outcome is that one can estimate the ACLFs after the modification has been made in a manner similar to that in conventional SEA.

Acknowledgement

The authors gratefully acknowledge the financial support provided by the Leverhulme Trust.

References

- [1] R.H. Lyon, R.G. DeJong, in: *Theory and Applications of Statistical Energy Analysis*, second ed., Butterworth-Heinemann, Boston, 1995.
- [2] C. Simmons, Structure-borne sound transmission through plate junctions and estimates of SEA coupling loss factors using the FE method, *Journal of Sound and Vibration* 144, 215–227 (1991).
- [3] G. Stimpson, N. Lalor, SEA extension of a F.E. model to predict total engine noise, *Internoise* 92 (1992) 557–560.
- [4] J.A. Steel, R.J.M. Craik, Statistical energy analysis of structure-borne sound transmission by finite element methods, *Journal of Sound and Vibration* 178 (1993) 553–561.
- [5] C.R. Fredö, SEA-like approach for the derivation of energy flow coefficients with a finite element model, *Journal of Sound and Vibration* 199 (1997) 645–666.
- [6] L. Maxit, J.L. Guyader, Estimation of SEA coupling loss factors using a dual formulation and FEM modal information—part II: numerical applications, *Journal of Sound and Vibration* 239 (2001) 931–948.
- [7] B.R. Mace, P.J. Shorter, Energy flow models from finite element analysis, *Journal of Sound and Vibration* 233 (2000) 369–389.
- [8] D.A. Bies, S. Hamid, In situ determination of loss and coupling loss factors by the power injection method, *Journal of Sound and Vibration* 70 (1980) 187–204.
- [9] F.F. Yap, J. Woodhouse, Investigation of damping effects on statistical energy analysis of coupled structures, *Journal of Sound and Vibration* 197 (1997) 351–371.
- [10] E.C.N. Wester, B.R. Mace, Statistical energy analysis of two edge-coupled rectangular plates: ensemble averages, *Journal of Sound and Vibration* 193 (1996) 793–822.
- [11] F.J. Fahy, A.D. Mohammed, A study of uncertainty in applications of SEA to coupled beam and plate systems—part 1: computational experiments, *Journal of Sound and Vibration* 158 (1992) 45–67.
- [12] B.R. Mace, J. Rosenberg, The SEA of two coupled plate: an investigation into the effects of subsystem irregularity, *Journal of Sound and Vibration* 212 (1998) 395–415.
- [13] C. Hopkins, Statistical energy analysis of coupled plate systems with low modal density and low modal overlap, *Journal of Sound and Vibration* 251 (2002) 193–214.
- [14] A.N. Thite, B.R. Mace, Robust estimation of coupling loss factors from finite element analysis, *Journal of Sound and Vibration* 303 (2007) 814–831.
- [15] B.R. Mace, Statistical energy analysis, energy distribution models and system modes, *Journal of Sound and Vibration* 264 (2003) 391–409.
- [16] B.R. Mace, Statistical energy analysis: coupling loss factors, indirect coupling and system modes, *Journal of Sound and Vibration* 279 (2005) 141–170.
- [17] R.R. Craig, *An Introduction to Computer Methods* John Wiley and Sons, 1981.
- [18] M.P. Castanier, Y.C. Tan, C. Pierre, Characteristic constraint modes for component mode synthesis, *AIAA Journal* 39 (6) (2001) 1182–1187.
- [19] Y.C. Tan, M.P. Castanier, C. Pierre, Power flow analysis of complex structures using characteristic constraint modes, *AIAA Journal* 43 (6) (2005) 1360–1370.
- [20] B.R. Mace, P.J. Shorter, A local modal/perturbational method for estimating frequency response statistics of built-up structures with uncertain parameters, *Journal of Sound and Vibration* 242 (2001) 793–811.